J Membrane Biol (2008) 223:59–72
DOI 10.1007/s00232-008-9114-8

ORIGINAL ARTICLES

A Mathematical Model of the Proton Balance in the Outer Mantle Epithelium of *Anodonta cygnea* L.

P. F. Oliveira · A. Rebelo da Costa · H. G. Ferreira

Received: 12 February 2008 / Accepted: 16 May 2008 / Published online: 28 June 2008

Abstract In the freshwater mollusc *Anodonta cygnea* and other unionids, the mantle plays an important role in the regulation of the movements of ions between the shell and the extrapaleal fluid. In this report, a mathematical model that attempts to describe the cell metabolic mechanisms underlying the operation of the outer mantle epithelium as a source of protons is presented. We encoded the information gathered by studying the epithelium in vitro, which includes the electrophysiology of the preparation, measurements of basic rates of transport of protons and base, the effect of metabolic and transport inhibitors on its electrical behavior and the dynamic measurements of pH_i. The model was conceived so that the short-circuit current (*I*sc) and fluxes of Na^+, K^+ and Cl^-; intracellular volume; electrical potential; and ionic concentrations can be computed as a function of time. Furthermore, the analytical descriptions of all ionic fluxes involved are such that the effect of transport inhibitors can be simulated. In all the simulations performed, it was possible to reproduce the experimental results obtained with specific inhibitors of transport systems on the *I*sc and on pH_i. In some cases, it was necessary to make alterations to one or more parameters of the reference condition. For each simulation carried out, the analysis of the results was consistent. The model is an analytical tool that can be used to show the internal coherence of the qualitative model previously proposed and to plan further experiments.

Keywords *Anodonta cygnea* · Bivalve · Freshwater · Short-circuit current · Mantle · pH_i · Voltage clamp · Berkeley Madonna · Proton transport

P. F. Oliveira · A. Rebelo da Costa
Laboratório Fisiologia dos Gâmetas e Transporte Iónico, Centro de estudos de ciência animal - Universidade do Porto (CECA - UP), Instituto de Ciências Biomédicas de Abel Salazar/ Laboratório nacional de investigação veterinária (ICBAS/ LNIV)—ala H, Rua dos Lagidos, Lugar da Madalena, 4485-655 VCD Porto, Portugal

A. Rebelo da Costa (✉)
Departamento Imuno-Fisiologia e Farmacologia, Instituto de Ciências Biomédicas de Abel Salazar, Universidade do Porto, Largo Abel Salazar, 2, 4099-003 Porto, Portugal
e-mail: a.rebelo@netcabo.pt

H. G. Ferreira
Rede de Química e Tecnologia (REQUIMTE), Departamento de Química, Faculdade de Ciências e Tecnologia (FCT), Universidade Nova de Lisboa, 2829-516 Caparica, Portugal

Introduction

Through the operation of a proton pump (V-ATPase) (Rebelo da Costa et al. 1999b), the outer mantle epithelium (OME) controls the pH of the extrapaleal fluid and, hence, the electrochemical gradient for calcium between its free and its crystallized forms (calcium carbonate) (Coimbra et al. 1992, 1993; Machado et al. 1990).

In this report, we present a mathematical model that attempts to describe the cell metabolic mechanisms underlying the operation of the epithelium as a source of protons.

We encoded the information gathered by studying the epithelium in vitro (Barrias 2003; Coimbra et al. 1988, 1992, 1993; Machado et al. 1990; Oliveira 2004; Rebelo da Costa 1999a, b), which includes the electrophysiology of the preparation, measurements of basic rates of transport of protons and base, the effect of metabolic and transport inhibitors on its electrical behavior and the dynamic measurements of pH_i.

Biological Structure: Compartments and Transport Systems

The system includes three very diluted aqueous spaces (Fig. 1): a cell compartment assumed to be a slab of 15 μm thickness and 1 cm^2 of cross section and two semi-infinite compartments, one on each side—the extrapaleal fluid and the hemolymph. Functionally, the preparation can be assumed, to a first approximation, to be transparent to calcium (Coimbra et al. 1988). The epithelium is represented by two barriers penetrated by ionic leaks. The barrier facing the shell side pumps protons from the cell interior to the extrapaleal fluid, and the barrier facing the hemolymph removes protons (or pumps bicarbonate) into the hemolymph compartment. The main source of protons and bicarbonate is the intracellular hydration of CO_2 metabolically produced. The hydration reaction is catalyzed by carbonic anhydrase (Coimbra et al. 1988; Machado et al. 1990).

The H^+ ions move to the shell side through a V-type proton pump (Oliveira et al. 2004; Rebelo da Costa et al. 1999b). This type of pump is specifically inhibited by bafilomycin A_1 and concanamycin A (Drose and Altendorf 1997). It was also described on the apical membrane of the cells of the turtle urinary bladder epithelium (Steinmetz and Andersen 1982) and the toad *Bufo marinus* (Ludens and Fanestil 1972), on the frog skin epithelium (Ehrenfeld et al. 1985), on the mantle of *Unio complanatus* (Hudson 1993), on mammalian renal collecting tubule (Gluck 1992) and on chick bone osteoclasts (Chatterjee et al. 1992).

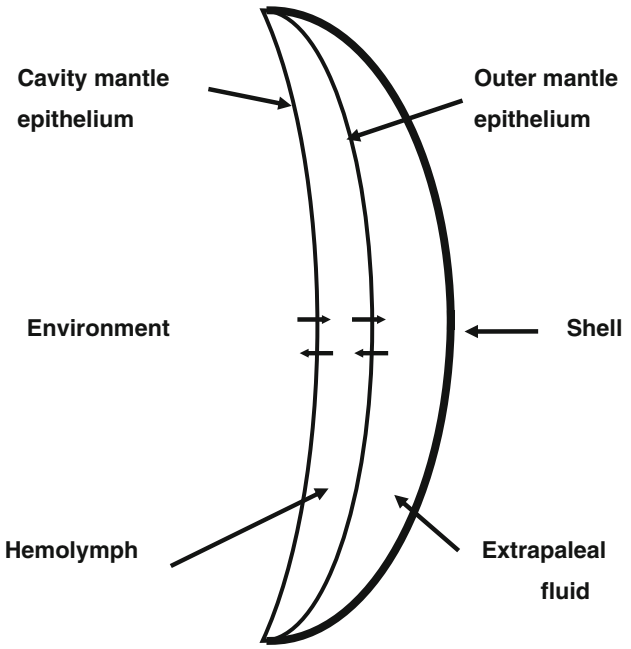

Fig. 1 Schematic representation of the mantle and the shell (one valve) of *Anodonta cygnea*

The movements of H^+ and HCO_3^- through the basolateral barrier of the OME cells are due to the presence of Na^+-dependent and Na^+-independent HCO_3^-/Cl^- exchangers, inhibited by 4−acetamido-4′-isothiocyanato-2,2′-stilbenedisulfonic acid (SITS) and 4,4′-diisothiocyanatostilbene-2,2′-disulfonic acid (DIDS), and a Na^+/H^+ exchanger, sensitive to amiloride (Coimbra et al. 1988).

The model was conceived so that the transepithelial short-circuit current and fluxes of Na^+, K^+ and Cl^-; intracellular volume; electrical potential; and ionic concentrations can be computed as a function of time. Furthermore, the analytical descriptions of all ionic fluxes involved are such that the effect of transport inhibitors can be simulated. The movements of calcium are not included because it was shown that they are entirely passive.

Methods

Description of the Model

A summary representation of the OME is reported in Fig. 2. Ions may cross the epithelium between the cells (shunt pathway, not represented) and through the cells

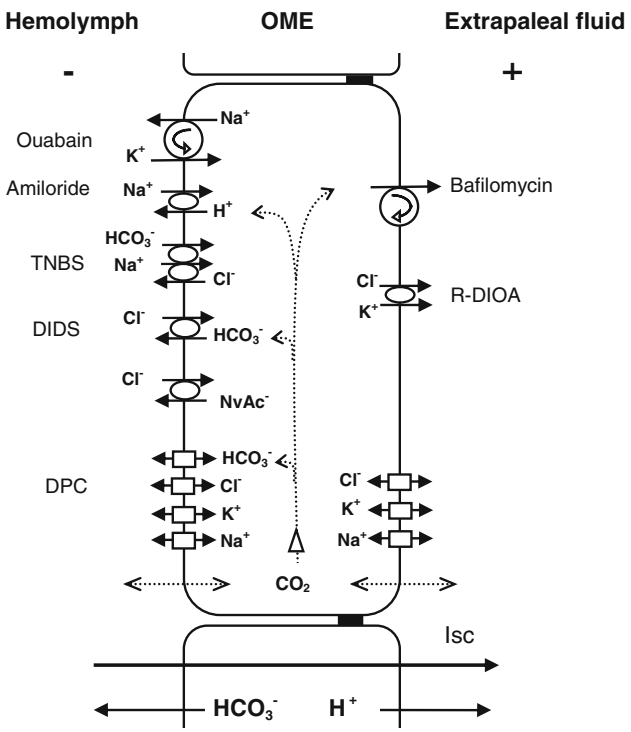

Fig. 2 Diagrammatic representation of the OME's membrane transport systems considered in the model (*triangles*, carbonic anhydrase; *ovals*, carriers; *rectangles*, channels; *circles*, pumps)

(cell pathway). The cell pathway consists of three components in series: the hemolymph and shell barriers separated by the cytoplasm. Both sides of the epithelium are bathed by aqueous, dilute, semi-infinite compartments. The intracellular compartment (cytoplasm) contains Na^+, K^+, Cl^-, bicarbonate, protons, nondiffusible ions (acting as buffers), nonvolatile acids and CO_2—all dissolved in water.

The core of the model is represented by a set of differential equations describing the mass conservation principle applied to the cell compartment and to each of the intracellular molecular species (Table 1). They are of the general form

$$d/dt(Qi) = \sum_c^h Ji - \sum_s^c Ji$$

which means the rate of change (d/dt) of the total amount (Q) of component i (Na^+, Cl^-, etc.) in the cell compartment (left side) is equal to the sum of the fluxes of component i (e.g., Na^+) from the hemolymph into the cell compartment minus the sum of the fluxes of component i from the cell into the shell compartment.

Table 1 Meaning of the symbols: notation 0 is used for the stationary state

[Cl⁻]cell	Cl^- intracellular concentration	*JK⁺_D*	Transcellular diffusional flux of K^+
[Cl⁻]hem/epf	Cl^- concentration in the hemolymph/extrapaleal fluid	*JK⁺_D_epf*	Diffusional flux of K^+ by the apical membrane
[CO₂]cell	CO_2 intracellular concentration	*JK_D_hem*	Diffusional flux of K^+ by the basolateral membrane
[CO₂]hem/epf	CO_2 concentration in the hemolymph/extrapaleal fluid	*JNa⁺_HCO₃⁻_hem*	Flux due to the $Na^+/HCO_3^-/Cl^-$ transporter
[H⁺]cell	Intracellular concentration of H^+	*JNa⁺_D*	Transcellular diffusional flux of Na^+
[H⁺]hem/epf	Concentration of H^+ in the hemolymph/extrapaleal fluid	*JNa⁺_D_epf*	Diffusional flux of Na^+ by the apical membrane
[HCO₃⁻]cell	Intracellular concentration of HCO_3^-	*JNa⁺_D_hem*	Diffusional flux of Na^+ by the basolateral membrane
[K⁺]cell	K^+ intracellular concentration	*Jp NvAc*	Metabolic production of nonvolatile acids
[K⁺]hem/epf	K^+ concentration in the hemolymph/extrapaleal fluid	*J NvAc_Cl⁻_hem*	Flux due to the fixed Acids/Cl^- exchanger
[Na⁺]cell	Na^+ intracellular concentration	*JpK⁺*	Flux of K^+ ion due to the Na^+/K^+ pump
[Na⁺]hem/epf	Na^+ concentration in the hemolymph/extrapaleal fluid	*JpNa⁺*	Flux of Na^+ ion due to the Na^+/K^+ pump
[NvAc]cell	Nonvolatile acids intracellular concentration	*JpNa⁺_M*	Maximum flux rate of the Na^+/K^+ pump
[OH⁻]cell	OH^- intracellular concentration	*P_CO₂*	Permeability of the cell to CO_2
[OH⁻]hem/epf	OH^- concentration in the hemolymph/extrapaleal fluid	*P_HCO₃⁻*	Permeability of the cell to HCO_3^-
[Prot⁻]_eq	Intracellular concentration of ionised proteins	*P_Cl⁻*	Permeability of the cell to Cl^-
[Prot]_mol	Total intracellular concentration of proteins	*P_K⁺*	Permeability of the cell to K^+
COsm	Osmolarity of the fluids	*P_Na⁺*	Permeability of the cell to Na^+
JCl⁻_D	Transcellular diffusional flux of Cl^-	*KK⁺_hem*	Affinity of the Na^+/K^+ pump to K^+
JCl_D_epf	Diffusional flux of Cl^- by the apical membrane	*KNa⁺_cell*	Affinity of the Na^+/K^+ pump to Na^+
JCl⁻_D_hem	Diffusional flux of Cl^- by the basolateral membrane	*Q NvAc*	Intracellular quantity of nonvolatile acids
JCl⁻_HCO₃⁻_hem	Flux due to the HCO_3^-/Cl^- exchanger	*Q CO₂T*	Total intracellular quantity of CO_2
JCl⁻_K⁺_epf	Flux due to the K^+/Cl^- transporter	*Q HCO₃⁻*	Intracellular quantity of HCO_3^-
JCO₂	Flux due to metabolic production of CO_2	*QH⁺T*	Total intracellular quantity of H^+
J CO₂_D	Total diffusional flux of CO_2	*QK⁺*	Intracellular quantity of K^+
JH⁺_Na⁺_hem	Flux due to the H^+/Na^+ exchanger	*QNa⁺*	Intracellular quantity of Na^+
JH⁺_Na⁺_hemM	Maximum flux rate of the H^+/Na^+ exchanger	*R*	Perfect gas constant
JH⁺_P	Flux due to the H^+ pump	*T*	Temperature in K
JH⁺_PM	Maximum flux rate of the H^+ pump	*TC*	Temperature in °C
J HCO₃⁻_D	Diffusional flux of HCO_3^-	*V_cell*	Cellular volume
J HCO₃⁻_P	Production of HCO_3^- by carbonic anhydrase	*Vm*	Membrane potential

There are six such equations (the seventh is excluded from electroneutrality). The *Qi* values are the primary intrinsic variables of the system. These values, with the exception of those at time zero, are generated by the model, i.e., cannot be modified directly. The fluxes *Ji* are computed from the corresponding kinetic equations. Under short-circuit conditions, the paracellular fluxes are zero; hence, the properties of the shunt do not influence the computations.

Since we have no available methods which allow the precise separate measurements of paracellular and transcellular fluxes, all the published quantitative information on the electrophysiology of the OME was obtained in vitro and under short-circuit conditions.

Diffusional Movements

It was assumed that the diffusional movements of Na^+, K^+ and Cl^- via the two barriers comply with the Goldman-Hodgkin-Katz equation. For each ion

$$Jdif = Pi \times \frac{\frac{zFV}{RT}}{\left[\exp\left(\frac{zFV}{RT}\right) - 1\right]} \times \left[C_1 \times \exp\left(\frac{zFV}{RT}\right) - C_2\right]$$

where *Jdif* is the diffusional flux of the *i* ion through the barrier (mol cm^{-2} s^{-1}), *Pi* is the permeability of the barrier to the *i* ion (cm s^{-1}), *z* is the valence of the ion (eq mol^{-1}), *F* is the Faraday constant (96,500 coul eq^{-1}), *V* is the transmembrane potential difference (volt), *R* is the gas constant (8,315 $Jmol^{-1}$ K^{-1}), *T* is the absolute temperature (273.15 + *T*°C, K) and C_1 and C_2 are the ion concentrations on both sides of the barrier (mol cm^{-3}).

We had to assume that both barriers had finite passive permeabilities for Na^+, K^+ and Cl^-. At the present stage the only data available on these "channels" are the isotopic measurements of Coimbra et al. (1988). Based on this indirect evidence, we chose, for each ion, to attribute a value to the permeability of a barrier expressed as a fraction of a global value, the remaining portion being attributed to the other barrier. These values were readjusted during the curve fitting of the model to the experimental results.

The total permeabilities for the potassium and chloride ions were calculated assuming that, in the steady state, the total entry flux of an ion into the cell is equal to the total exit flux of the same ion. It was further assumed that, for both these ions, the permeability of the shell membrane is distinct from the permeability of the hemolymph membrane.

A low value was attributed to the transcellular permeability of the Na^+ ion (Coimbra et al. 1988). It was also assumed that, for this ion, the permeability of the shell membrane is different from the permeability of the hemolymph barrier (Coimbra et al. 1988).

The diffusional flux of carbon dioxide through cellular membranes occurs by simple diffusion and is described by the following equation:

$$JCO_2\_Dif = P\_CO_2 \times ([CO_2]Hem\_[CO_2])$$

ATPases

The flux of protons due to the proton pump is provided by the equation

$$JH^+\_P = JH^+\_PM \times \left(\frac{[H^+]cell}{[H^+]cell + KH^+\_cell}\right)$$

where JH^+_P is the flux of the ion via the proton pump, $JH^+\_P_M$ is the flux of the ion at saturation and $K\,H^+\_cell$ is the affinity of the pump to the H^+ ion.

The flux of sodium due to the Na^+/K^+ pump is provided by the equation (Hoffman and Tosteson 1971)

$$JpNa^+ = JpNa^+\_M\left(\frac{[Na^+]cell}{[Na^+]cell + KNa^+\_cell}\right)^3 \times \left(\frac{[K^+]hem}{[K^+]hem + KK^+\_hem}\right)^2$$

where $JpNa^+$ is the Na^+ flux via the Na^+/K^+ pump, $JpNa^+\_M$ is the Na^+ flux at saturation, KK^+_hem is the affinity of the Na^+/K^+ pump to the K^+ ion on the hemolymph side and KNa^+_cell is the affinity of the Na^+/K^+ pump to the Na^+ ion on the cytoplasm side.

Membrane Transporters

For the transport processes for which detailed kinetic information is missing, first-order kinetics were assumed and the flux couplings were represented by the products of the concentrations of the coupled ions, in the same compartments (for cotransports) or in opposite compartments (for contratransports).

For the Na^+/H^+, HCO_3^-/Cl^- and $NvAc/Cl^-$ exchangers, the general form of the equation is as follows:

$$Jxy = Jxy_M \times (Cx\_1 \times Cy\_2 - Cx\_2 \times Cy\_1)$$

For the $Na^+/HCO_3^-/Cl^-$ carrier, the general form of the equation is as follows:

$$Jxyz = Jxyz_M \times (Cx\_1 \times Cy\_1 \times Cz\_2 - Cx\_2 \times Cy\_2 \times Cz\_1)$$

For the K^+/Cl^- carrier, the form of the equation is

$$Jxy = Jxy_M \times (Cx\_1 \times Cy\_1 - Cx\_2 \times Cy\_2)$$

where *Jxy* is the flux via the *X/Y* transporter, *Jxyz* is the flux via the *X/Y/Z* transporter, Jxy_M is the flux at saturation via the *X/Y* transporter, $Jxyz_M$ is the flux at saturation via the *X/Y/Z* transporter, *Cx_1* and *Cx_2* are the concentrations of

the *x* ion on both sides of the membrane, *Cy_1* and *Cy_2* are the concentrations of the *y* ion on both sides of the membrane and *Cz_1* and *Cz_2* are the concentrations of the *z* ion on both sides of the membrane.

Computational Strategy

The model is run by solving it first for the steady state (when all the *d/dt* [*Qi*] values are equal to zero). The set of differential equations is thus converted into a set of non-linear simultaneous equations which is solved sequentially.

We start by choosing the initial values of the variables for which there is published information (Table 2). It was assumed that the extracellular fluids (extrapaleal fluid and hemolymph) were identical in composition and included sodium, potassium, chloride, calcium, protons, hydroxyl and bicarbonate ions, carbon dioxide and nonvolatile ionized acids (assumed to have a valence of −1) and ionized proteins.

The ionized fixed bases are supposed to result from the metabolic production of nonvolatile acids (phosphoric acid, sulfuric acid, etc.) and organic acids produced by the intermediary metabolism.

While the ionic concentrations in the extracellular compartments were measured directly, the intracellular concentrations were chosen from published experimental data (Coimbra et al. 1988, 1992) so as to obtain a steady situation. The intracellular electrical potential was assumed to be −40 m*V*, in agreement with the results of Coimbra et al. (1992).

Then, for a membrane potential of 40 m*V*, the quotients of the dominant ions, $[K^+]cell/[K^+]epf/hem$ and $[Cl^-]cell/[Cl^-]\_epf/hem$, must be greater than

$$\exp\left[ZFV/(RT)\right] \cong 4,8$$

Intracellular concentrations of 40 and 3.2 mM were chosen for K^+ and Cl^-, respectively. This choice was determined in simulations of the steady state with $V_m = -40$ m*V*, on the one hand, and, on the other, with all the parameters of the model (permeabilities, affinities, maximum rates, etc.) being positive.

The contribution of the Na^+ diffusion potential to the membrane potential seems to be small (Coimbra et al. 1988). It is to be expected that, as a consequence of the sodium pump operation, it will contribute to the membrane potential with a positive Nernst potential.

The intracellular concentration of bicarbonate is computed, on the one hand, from the balance between the production of carbon dioxide and its diffusion out of the cell and, on the other, from the speed at which it is

Table 2 Stationary state values of variables and parameters

V_cell_0	1.5 e^{-3}	$cm^3\ cm^{-2}$	P_K^+	8.5 e^{-5}	$cm\ s^{-1}$
[H+]hem/epf	3.9811 e^{-11}	$mol\ cm^{-3}$	P_Cl^-	3.5 e^{-3}	$cm\ s^{-1}$
$[OH^-]hem/epf$	7.862 e^{-10}	$mol\ cm^{-3}$	$P\_HCO_3^-$	3.3 e^{-4}	$cm\ s^{-1}$
$[K^+]hem/epf$	7.0 e^{-6}	$mol\ cm^{-3}$	$JNvAc\_Cl^-\_hem\_0$	−2.0 e^{-11}	$mol\ cm^{-2}\ s^{-1}$
$[Na^+]hem/epf$	18.0 e^{-6}	$mol\ cm^{-3}$	JCO_2_0	2.0 e^{-9}	$mol\ cm^{-2}\ s^{-1}$
$[Cl^-]hem/epf$	17.0 e^{-6}	$mol\ cm^{-3}$	$J\ CO_2\_D\_0$	−5.8 e^{-9}	$mol\ cm^{-2}\ s^{-1}$
$[CO_2]hem/epf$	0.8913 e^{-6}	$mol\ cm^{-3}$	$J\ HCO_3^-\_D\_0$	−8.6 e^{-11}	$mol\ cm^{-2}\ s^{-1}$
$[HCO_3^-]hem/epf$	10.0 e^{-6}	$mol\ cm^{-3}$	$J\ HCO_3^-\_P\_0$	2.0 e^{-10}	$mol\ cm^{-2}\ s^{-1}$
[NvAc]hem/epf	1.0 e^{-6}	$mol\ cm^{-3}$	$JCl^-\_HCO_3^-\_hem\_0$	1.29 e^{-10}	$mol\ cm^{-2}\ s^{-1}$
$[H^+]cell\_0$	1.585 e^{-10}	$mol\ cm^{-3}$	*JCl_D_0*	−1.25 e^{-10}	$mol\ cm^{-2}\ s^{-1}$
$[OH^-]cell\_0$	1.975 e^{-10}	$mol\ cm^{-3}$	*JCl_D_epf_0*	−3.7 e^{-11}	$mol\ cm^{-2}\ s^{-1}$
$[K^+]cell\_0$	40.0 e^{-6}	$mol\ cm^{-3}$	$JCl^-\_D\_Hem\_0$	−8.7 e^{-11}	$mol\ cm^{-2}\ s^{-1}$
$[Na^+]cell\_0$	2.0 e^{-6}	$mol\ cm^{-3}$	$JCl^-\_K^+\_epf\_0$	1.0 e^{-11}	$mol\ cm^{-2}\ s^{-1}$
$[Cl^-]cell\_0$	3.2 e^{-6}	$mol\ cm^{-3}$	$JH^+\_P\_0$	2.0 e^{-10}	$mol\ cm^{-2}\ s^{-1}$
$[CO_2]cell\_0$	0.897 e^{-6}	$mol\ cm^{-3}$	$JK^+\_D\_0$	−8.6 e^{-11}	$mol\ cm^{-2}\ s^{-1}$
$[HCO_3^-]cell\_0$	2.0 e^{-6}	$mol\ cm^{-3}$	$JK^+\_D\_epf\_0$	−1.7 e^{-11}	$mol\ cm^{-2}\ s^{-1}$
[NvAc]cell_0	1.0 e^{-6}	$mol\ cm^{-3}$	$JK^+\_D\_hem\_0$	−6.9 e^{-11}	$mol\ cm^{-2}\ s^{-1}$
$[Prot^-]\_eq\_0$	2.83 e^{-5}	$mol\ cm^{-3}$	$JNa^+\_HCO_3^-\_hem\_0$	1.4 e^{-11}	$mol\ cm^{-2}\ s^{-1}$
KNa^+_cell	2.0 e^{-7}	$mol\ cm^{-3}$	$JNa^+\_D\_0$	109 e^{-12}	$mol\ cm^{-2}\ s^{-1}$
KH^+_cell	1.585 e^{-10}	$mol\ cm^{-3}$	$JNa^+\_D\_epf\_0$	1.6 e^{-11}	$mol\ cm^{-2}\ s^{-1}$
KK^+_hem	1.0 e^{-6}	$mol\ cm^{-3}$	$JNa^+\_D\_hem\_0$	9.3 e^{-11}	$mol\ cm^{-2}\ s^{-1}$
KCO_2	6.0 e^{-6}	$mol\ cm^{-3}$	*JpNvAc_0*	2.0 e^{-11}	$mol\ cm^{-2}\ s^{-1}$
Vm_0	0.043	*V*	JpK^+_0	96 e^{-12}	$mol\ cm^{-2}\ s^{-1}$
P_Na^+	3 e^{-6}	$cm\ s^{-1}$	$JpNa^+\_0$	143 e^{-12}	$mol\ cm^{-2}\ s^{-1}$

hydrated by the carbonic anhydrase (Maren 1967). Given the extremely high permeability of biological membranes to carbon dioxide, an appreciable gradient of the concentrations of this gas between the intracellular and extracellular compartments is not to be expected. The concentration of intracellular carbon dioxide used in the reference condition was around 1% higher than the external concentration. For an external pH of 7.4 and a concentration of bicarbonate of 10 mM, the extracellular concentration of CO_2 is around 0.9 mM. The intracellular concentration of CO_2 and the pH_i of 6.8 enable us to estimate the equilibrium intracellular concentration of bicarbonate as 2.5 mM. In order to maintain a continuous production of bicarbonate, we accepted its concentration as being below its equilibrium value (2 mM). Unless values arise which are very different from these, their choice will not greatly affect the behavior of the model.

The total quantity of proteins in the cell was considered fixed and is provided by the principle of isotonicity of fluids ($Cosm_{intracellular} = Cosm_{extracellular}$). Therefore,

$$\begin{aligned}[\text{Prot}]\_\text{mol} &= \text{COsm}\_0 - [\text{Na}^+]cell\_0 - [K^+]cell\_0 \\ &- [H^+]cell\_0 - [HCO_3^-]cell\_0 - [Cl^-]cell\_0 \\ &- [OH^-]cell\_0 - [NvAc]cell\_0\end{aligned}$$

The quantity of ionized proteins in the cell, in the steady state, is provided by the electroneutrality equation:

$$\begin{aligned}[\text{Pr}\,ot]\_eq\_0 = {} & [Na^+]cell\_0 + [K^+]cell\_0 + [H^+]cell\_0 \\ & - [HCO_3^-]cell\_0 - [Cl^-]cell\_0 \\ & - [OH^-]cell\_0 - [NvAc]cell\_0\end{aligned}$$

The ionization of the intracellular proteins as a function of pH was assumed to follow the relation proposed by Van Slyke and Sendroy (1928) for plasma proteins:

$$\{Pr^- = A \times (pH - pK_{\text{Pr}})\}$$

where pK_{Pr} is the isoelectric pH. We did not find published experimental values of pK_{Pr} and arbitrarily decided to use a value (6.0) intermediate between those of serum albumin (4.9) and hemoglobin (7.1). We repeated all the simulations to be presented later using a range of intermediate values between 5 and 7 and obtained negligible variations in the estimated parameters, which did not influence the conclusions to be drawn.

The values for the fixed base intracellular concentrations were arbitrarily chosen as 1 mM. The use of the model will take care of providing adjustments for the values chosen.

Until we have more specific probes for identifying transport systems, we will have to use coarser methods. In this specific case, a combination of three criteria was used:

1. The use of specific inhibitors of transport as indicators of the presence of a transporter;
2. The detection of a variation in the short-circuit current as an indication of an effect;
3. The side of the epithelium where the inhibitor had an effect as an indicator of the barrier where the transporter is located.

Using these three criteria, the following transport systems were considered, which are illustrated in Fig. 2:

1. H^+-ATPase V-type (shell barrier) (Rebelo da Costa et al. 1999b)
2. Na^+-K^+ pump (hemolymph barrier) (Rebelo da Costa et al. 1999a)
3. Na^+/H^+ transporter (hemolymph barrier) (Coimbra et al. 1988)
4. $Na^+/HCO_3^-/Cl^-$ transporter (hemolymph barrier) (Barrias 2003)
5. HCO_3^-/Cl^- transporter (hemolymph barrier) (Coimbra et al. 1988)
6. Cl^- channels (shell and hemolymph barriers) (Barrias 2003)
7. K^+/Cl^- transporter (shell barrier) (Rebelo da Costa 1994)

Given the presence of the Na^+/K^+ pump, it was necessary to postulate the presence of

8. Na^+, K^+ channels (shell and hemolymph barriers).

It is not very plausible that the production of anions results exclusively from the hydration of CO_2, so we assumed a production of nonvolatile acids and consequently a:

9. nonvolatile acid/Cl^- transporter (hemolymph barrier).

Transporters for nonvolatile organic bases have been extensively studied in the mammalian kidney (Stephen and Dantzler 2003) as well as exchange anion transporters for sulfate (Markovich 2001) and phosphate (Murer et al. 2000)—hence our justification for including them, albeit in a very general way in our system.

The introduction of

10. HCO_3^- channels (hemolymph barrier)

arose from the observation that the model was unstable when the HCO_3^-/Cl^- exchanger was inhibited.

Principles of Conservation

The resolution of the model entails stipulating a set of relations which will allow a reduction in the degrees of freedom of the system. The starting point is to stipulate the steady state defined by

$$d/dt(Qi) = 0$$

where Qi is the total intracellular amount of the component i. Under these conditions, for each ion i and in a steady state:

$$\sum Ji = 0$$

i.e., the total sum of the fluxes of a component i via the barriers of the cell compartment is nil (there is no accumulation or depletion). There will be a system of six simultaneous equations which will only enable six parameters to be computed.

We used a set of additional relations which allow the remaining parameters to be calculated:

1. *Isotonicity* – This enabled the amount of osmotically active proteins in the steady state to be ascertained. It was considered that this would remain constant in any experimental situation. It was also assumed that the movements of water via the cellular barrier are sufficiently quick so that if there are any changes in the intracellular composition, the isotonicity is instantaneously maintained, at the cost of changes to the cellular volume.
2. *Conservation of mass* – The rate of accumulation of a given component in the cellular compartment is due to the difference between the influx via the hemolymph barrier and the efflux via the shell barrier. This principle enabled us to stipulate the maximal transport rates in the reference condition.
3. *Electroneutrality* – The net charge of the cell compartment (as well as the outside compartments) is always zero. This assumption enabled us to compute the instantaneous values of the intracellular chloride ion. This assumption is an approximation since across both barriers there will be a charge separation, hence a net charge in the two thin adjacent unstirred layers on both sides of the two barriers.
4. We assumed relations between certain fluxes based on the observations of the effect of inhibitors.

The Steady State

Since the majority of experimental observations were made under short-circuit conditions, the paracellular fluxes were always zero and are therefore not considered in the model. A number of ionic fluxes were postulated:

1. *Flux of protons*: Using the results described by Coimbra et al. (1988) and by Rebelo da Costa et al. (1999b) as a starting point, where the short-circuit current generated by the EEM was shown to be due to the flux of protons from the hemolymph to the extrapaleal fluid, generated by the action of a V-type proton pump, this flux was set at an initial value corresponding to the average (or typical) value of the short-circuit currents measured. Thus,

$$J[H^+]\_P\_0 = 2.1 \times 10^{-10} mol \times cm^{-2} \times s^{-1}$$

The total production of H^+ in the cell was assumed to result from the operation of the Na^+/H^+ transporter, the H^+ pump, and the generation of H^+ derived from the formation of nonvolatile acids (*JpNvAc*) and of the bicarbonate ion (*JBic_P*) by the cell. In the steady state, according to the mass conservation principle, the production of protons is equal to their extrusion from the cell via the proton pump and the H^+/Na^+ exchanger. Thus, in the steady state:

$$JpNvAc\_0 + JHCO_3^-\_P\_0 - JH^+\_Na^+\_hem\_0 = JH^+\_P\_0$$

2. *Production of carbon dioxide*: The choice of a value for the production of CO_2 is arbitrary. It is possible to set a lower limit to it, corresponding to the rate at which the protons are expelled from the shell side. This value was chosen to allow simulations whereby the proton pumping rate increases:

$$JCO_2 = 2.0 \times 10^{-9} mol \times cm^{-2} \times s^{-1}$$

With this choice, the production of CO_2 is never a factor which restricts the operation of the system.

3. *Flux of the bicarbonate ion*: Based on the results described by Machado et al. (1990), confirmed by Hudson (1992) in *Unio*, the short-circuit current generated by the OME is numerically equal to the flux of bicarbonate ions via the hemolymph barrier. In principle, this flux should be numerically equal to the flux of bicarbonate ions produced in the cell by the action of carbonic anhydrase ($JHCO_3^-\_P$) so that, in the steady state, the concentration of the intracellular bicarbonate is constant. An initial value corresponding to the value of the short-circuit current was attributed to the production of bicarbonate:

$$JHCO_3^-\_P\_0 = JH^+\_P = 2.0 \times 10^{-9} mol \times cm^{-2} \times s^{-1}$$

Based on the effects observed with bicarbonate transport blockers, we assumed that the flux of this ion via the hemolymph barrier is due to the action of two types of transporter, a $Na^+/HCO_3^-/Cl^-$ transporter and a HCO_3^-/Cl^- transporter. As stated above, in order to stabilize the model, it was necessary to assume the existence of bicarbonate channels which have already been observed in other systems (Cabantchik and Greger 1992; Mason et al. 2003). Thus, the sum of the bicarbonate fluxes in the

steady state, due to each of these transport mechanisms, is equal to:

$$JNa^+\_HCO_3^-\_Hem\_0 - JCl^-\_HCO_3^-\_Hem\_0 + JHCO_3^-\_D\_0 = -JHCO_3^-\_P\_0$$

4. *Flux of sodium ion*: The total flux of sodium via both barriers is due to the action of the Na^+/H^+ transporter, the $Na^+/HCO_3^-/Cl^-$ transporter, Na^+ channels and the Na^+/K^+ pump. In the steady state, according to the mass conservation principle, the entry flux of sodium into the cell is equal to the exit flux. Thus,

$$JNa^+\_HCO_3^-\_Hem\_0 + JH^+\_Na^+\_Hem\_0 + JNa^+\_D\_0 = JpNa^+\_0$$

The flux of sodium via the $Na^+/HCO_3^-/Cl^-$ transporter, in the steady state, is calculated as a fraction of the Na^+ flux via the Na^+/K^+ pump:

$$JNa^+\_HCO_3^-\_Hem\_0 = 0.1JpNa^+\_0$$

There are no data regarding the value of this flux; therefore, the value chosen is arbitrary so as not to exert too much influence on the simulations, although enabling the effect of inhibitors to be simulated.

Exactly the same considerations were used for calculating the flux of sodium via the Na^+/H^+ transporter, in the steady state:

$$JH^+\_Na^+\_Hem\_0 = 0.1JH^+\_P\_0$$

5. *Flux of potassium ion*: The total flux of potassium across the cell compartment is the algebraic sum of the flux through the Cl^-/K^+ transporter (shell barrier) and the K^+ channels and the Na^+/K^+ pump (hemolymph barrier). In the steady state, according to the mass conservation principle, the entry flux of potassium into the cell is equal to the exit flux. Thus,

$$JpK^+\_0 + JK^+\_D\_0 - JCl^-\_K^+\_Ep\_0 = 0$$

Since the transport stoichiometry (3/2) of the Na^+/K^+ pump (3 Na^+ ions outward for 2 K^+ ions inward) is

$$JpK^+\_0 = -(2/3) \times JpNa^+\_0$$

The diffusional flux of potassium, in the steady state, corresponds to the arbitrary sharing of the K^+ flux via the pump among the K^+ channel and the Cl^-/K^+ transporter.

6. *Flux of nonvolatile acids*: The total flux of nonvolatile acids via the hemolymph barrier is due to the intracellular production of these acids and to the action of the nonvolatile acid/Cl^- transporter. In the steady state and according to the mass conservation principle, the production of nonvolatile acids in the cell is equal to the exit flux. Thus,

$$JpNvAc\_0 + JNvAc\_Cl^-\_Hem\_0 = 0$$

7. *Flux of chloride ion*: The total flux of chloride ion through the cell compartment is due to the action of the $Na^+/HCO_3^-/Cl^-$ transporter (hemolymph barrier), the K^+/Cl^- transporter, the HCO_3^-/Cl^- transporter and Cl^- channels. In the steady state, according to the mass conservation principle, the entry flux of chloride ions into the cell is equal to the exit flux. Thus,

$$-JCl^-\_HCO_3^-\_Hem\_0 + JNa^+\_HCO_3^-\_Hem\_0 - JNvAc\_Cl^-\_Hem\_0 + JCl^-\_D\_0 = JCl^-\_K^+\_Ep\_0$$

The computation of the ionic fluxes (for Na, K and Cl) across the two barriers started with an estimation of the cell permeability to these ions (*P_Na*, *P_K* and *P_Cl*) based on the measurements of unidirectional fluxes by Coimbra et al. (1988). In the same report, the response of the intracellular potential to external variations of the concentrations of the two gives an indication of the relative permeabilities of the two barriers. The ratio of the two permeabilities for each ion was then relaxed during the curve fitting.

The Dynamic Model

The dynamic behavior of the model is described by the solution of the following differential equations (the principle of electroneutrality is used to remove the equation for *QCl*):

$$\begin{aligned} d/dt(QNa) &= JNa^+\_D + JH^+\_Na^+\_hem + JNa^+\_HCO_3^-\_hem - JpNa^+ \\ d/dt(QK) &= JpK^+ + JK^+\_D - JCl^-\_K^+\_epf \\ d/dt(QAnCarbT) &= JAnCarb - JCl^-\_HCO_3^-\_hem + JNa^+\_HCO_3^-\_hem + JAnCarb\_D + JHCO_3^-\_D \\ d/dt(QHidT) &= JpNvAc - JH^+\_P + JHCO_3^-\_P - JH^+\_Na^+\_hem \\ d/dt(QAcNv) &= JpNvAc + JNvAc\_Cl^-\_hem \\ d/dt(QBic) &= JHCO_3^-\_P + JNa^-\_HCO_3^-\_hem - JCl^-\_HCO_3^-\_hem + JHCO_3^-\_D \end{aligned}$$

The calculation strategy consists of calculating the $Qi(t+\Delta t)$ value based on the $Qi(t)$ and the *d/dt (Qi[t])* value. The calculation method used is provided by the Berkeley Madonna application software (www.berkeley madonna.com, generously supplied by Prof. Robert Macey), which allows a choice between five algorithms. The choice is made empirically, using the simple criteria of selecting the method which will most rapidly produce results within the error stipulated.

Results

Simulations

The computational strategy used in simulating the effect on the short-circuit current (*I*sc) and pH_i of the OME of specific inhibiting substances of membrane transport systems consisted of altering the value of one or more parameters as described below. The parameters chosen are an interpretation of the effects of the inhibitors in terms of the model.

The perturbations introduced into the model followed a generic design:

- The blocking of channels is simulated by decreasing the value of the corresponding permeability.
- The blocking of the pumps and transporters is simulated by decreasing the values of the corresponding maximal rates of transport.

In order to prevent numerical discontinuities, the values of the parameters were never decreased to zero and the transitions between the values of the parameters were exponential, using expressions of the following type:

$$PAR(t) = PAR(0) * (1 - \exp[-t/\tau])$$

where *PAR(t)* and *PAR(0)* are the values of the factor that multiply the parameter to be perturbed at the instants *0* and *t* and τ is a time constant. *PAR(t)* is thus a time-smoothing function. The response of the *I*sc of the OME to the inhibitors is generally very slow. The effect of any drug on *I*sc is a chain of events, which include its diffusion to the respective receptor (via an unstirred layer), its combination with the receptor and the effect of this combination on the processes which follow and on ionic transport via the two barriers. All these mechanisms occur in accordance with the respective rates, which are unknown at this time.

Since all the underlying processes that lead to the generation of short-circuit current are computed, we can use the numbers generated relating to fluxes, intracellular concentrations and cell volume and intracellular electrical potential to explain the effect of transport inhibitors. Table 3 reports the values chosen in the following descriptions. The aim of this table was to show which of the model variables were affected by the inhibitors used. Presentation of the original data would need a much larger table with the same purpose. To obtain their absolute values, they have to be multiplied by the corresponding values of Table 2. Any evaluation of the model short of a

Table 3 Variation of the values of concentration, pH_i, cellular volume and fluxes of the different transport systems resulting from the effect of the inhibitors on *I*sc and pH_i (*)

	Amilo	Bafilo	Diamox	DIDS	SITS	DIOA	Ouabain	Amilo*	Bafilo*
V_m							−0.39		
V_cell			0.98			0.21	0.56		
pH_cell									
$[Cl^-]cell$						0.35	0.91		
$[Na^+]cell$	−0.57		−0.44	−0.26	−0.26	−0.22	9.2	−0.91	
$[K^+]cell$							−.5		
$[HCO_{3-}^-]cell$				0.27	0.2	0.33	0.84		
$JpNa^+$	−0.29						−0.7	−0.87	
JpK^+	−0.29						−0.7	−0.87	
JH^+_P		−0.94	−0.84				−0.26		−0.99
$JHCO_{3-}^-\_D$									
$JHCO_{3-}^-\_P$		−0.92	−0.93				−0.34	−0.8	−1.38
$JH^+\_Na^+\_hem$	−0.85	0.28	−0.93			−0.22	−0.68	−0.97	0.4
$JNa\_HCO_{3-}^-\_hem$				−0.98	−0.97	0.4	−1.34		
$JCl^-\_HCO_{3-}^-\_hem$		−0.74		−0.39	−0.47		−0.37	−0.76	−1.25
$JCl^-\_K^+\_epf$	−0.24		−0.86			−0.63	−0.6	−0.8	
$JNvAc\_Cl^-\_hem$									
$JHCO_{3-}^-\_D$		−0.77	−1.1				−0.49	−0.7	−1.2
Jna^+_D	−0.3						−0.53	−0.95	
JK^+_D	−0.29		0.49			4.73	−0.7	−0.85	
JCl^-_D	0.57	−1.13	−14.63		−0.27	0.71	−0.21		−0.71

Values are the ratio between the shift from the stationary state (final value minus stationary value), due to inhibitory effect, and the value at the stationary state

Amilo, amiloride; Bafilo, bafilomycin

numerical simulation cannot be performed without these data.

In order to reduce the extension of the text, others left out were considered less relevant.

Effect of Amiloride on Ccc

Amiloride is a specific inhibitor of the Na^+/H^+ exchanger (Grinstein and Smith 1987; Mahnensmith and Aronson 1985), and its inhibitory action on specific Na^+ membrane channels has also been described (Benos et al. 1987). Its effect on the *I*sc of the OME was described by Coimbra et al. (1988) and was simulated by reducing the maximum rate of transport of the Na^+/H^+ exchanger by 98% and the permeability of the basolateral membrane to the Na^+ by an identical amount. The time course of the experimental and computed values of *I*sc is reported in Fig. 3a, where the solid line represents the simulation and the dotted line is the *I*sc recording.

In order to simulate this effect, we had to increase the reference values of permeability to the Na^+ ion of both epithelial barriers and decrease the fraction of bicarbonate ion transported by the $Na^+/HCO_3^-/Cl^-$ transporter.

Coimbra et al. (1988) attributed the effect of this inhibitor on *I*sc to the inhibition of the Na^+/H^+ exchanger. Our simulation points to the existence of Na^+ channels sensitive to this inhibitor.

In Table 3, column 2, we can see that by reducing the maximum rate of transport of the Na^+/H^+ exchanger there is a direct decrease in the flux of H^+ and Na^+ ions via this transport system ($JH^+\_Na^+\_hem$). The decrease in the exit of H^+ ions from the cell leads to an increase of its intracellular concentration, which implies a slight rise in its flux via V-ATPase (JH^+_P). The reduced Na^+ entry flux leads to a decrease in the rate of transport of the Na^+/K^+ pump ($JpNa^+$)—hence the decrease in the diffusional flux of these ions via their specific channels (JNa^+_D e JK^+_D).

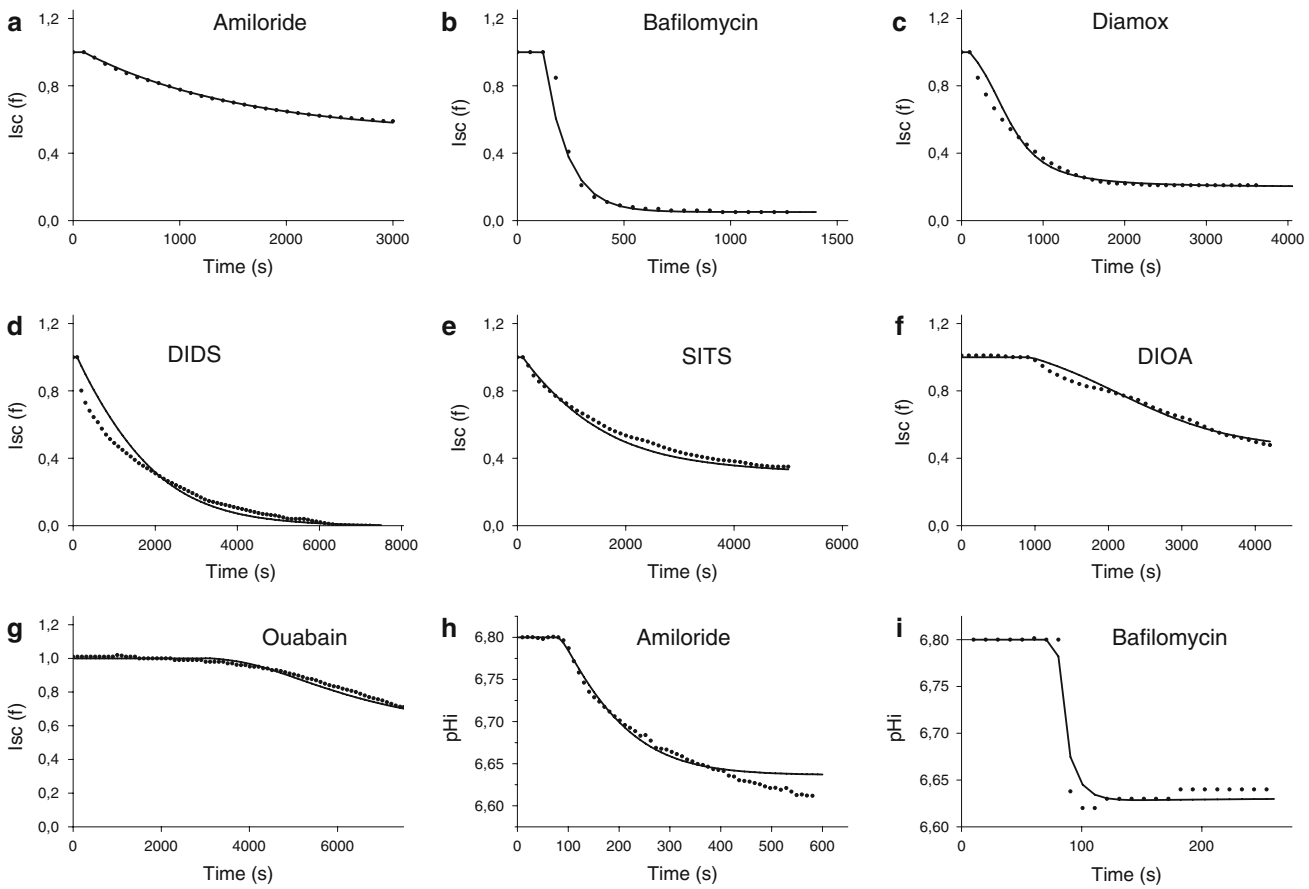

Fig. 3 Effect of inhibitors on *I*sc (fractional value) (**a**–**g**) and on pH_i (**h, i**). Experimental values (*circles*) and values resulting from the model computation (*lines*)

Effect of Bafilomycin A_1 on *I*sc

Bafilomycin A_1 is a specific inhibitor of V-ATPases (Drose and Altendorf 1997). Its effect on the *I*sc was studied by Rebelo da Costa et al. (1999b) These authors noted that the current was inhibited when they added bafilomycin A_1 to the apical side of the epithelium. Its effect was simulated by reducing the maximum pumping rate of V-ATPase by 95%. The experimental values and those resulting from the simulation are represented in Fig. 3b, while Table 3, column 3, represents the variation of the fluxes of the different transport systems with the application of the inhibitor. There is no significant discrepancy between the values computed and the experimental values for this simulation.

As we can see in Table 3, column 3, by reducing the maximum rate of transport of V-ATPase, there is a direct decrease of the flux of H^+ ions via this pump (JH^+_P) and a consequent increase in its concentration. This implies a shift to the left (CO_2 production) of the CO_2 hydration reaction, a reduction in the intracellular concentration of the bicarbonate ion ($JHCO_3^-\_P$) and an increase in the rate of transport of the Na^+/H^+ exchanger ($JH^+\_Na^+\_Hem$). The decrease of the intracellular bicarbonate ion in turn leads to a reduction in its flux via the specific channels ($J\ HCO_3^-\_P\_D$) and of the HCO_3^-/Cl^- exchanger ($JCl^-\_HCO_3^-\_Hem$). The decrease in the diffusional flux of chloride (JCl^-_D) can only be explained by the slight depolarization of the intracellular compartment.

Effect of Diamox on *I*sc

Acetazolamide (Diamox) is a specific inhibitor of carbonic anhydrase (Ashe et al. 1956; Enns and Hill 1983). The effect of this substance on *I*sc of the OME was studied by Coimbra et al. (1988), using the voltage-clamp technique. These authors noted that the current was inhibited when they added Diamox to either side of the epithelium. Its effect was simulated by reducing the maximal rate of activity of the enzyme by 98.5%. The experimental values and those resulting from the simulation are represented in Fig. 3c. The variation of the fluxes of the different transport systems after the application of Diamox is represented in Table 3, column 4.

In order to simulate the effect of Diamox, we did not need to make any alteration to the parameters and initial fluxes.

By analyzing the most significant variations in the fluxes considered, we can see (Table 3, column 4) that by reducing the maximal rate of hydration of carbon dioxide ($J\ HCO_3^-\_P$), there is a direct drop in the intracellular production of bicarbonate and H^+ ions and consequent reductions in the intracellular concentrations of protons and bicarbonate and of the exit fluxes of these ions from the cell, due to the decrease in the rate of transport of the Na^+/H^+ exchanger ($JH^+\_Na^+\_hem$) and of the proton pump (JH^+_P). The decrease of the intracellular bicarbonate ion in turn leads to a decreased flux of the bicarbonate ion via the specific channels ($J\ HCO_3^-\_D$) and the HCO_3^-/Cl^- exchanger ($JCl^-\_HCO_3^-\_hem$). The drop in the rate of transport of the HCO_3^-/Cl^- exchanger reduces the entry of Cl^- ion into the cell and, thus, entails a decrease in its diffusional flux (JCl^-_D).

Effect of DIDS and SITS on *I*sc

Both DIDS and SITS inhibit the $Na^+/HCO_3^-/Cl^-$ and HCO_3^-/Cl^- transporters (Boron and Boulpaep 1983; Pace et al. 1983) and specific Cl^- membrane channels (Bicho et al. 1999; Jensen and Skott 1996). The effect of these inhibitors on *I*sc was described by Coimbra et al. (1988) and is shown in Fig. 3d, e. When the inhibitor was added to the basolateral side, they noted a decrease in *I*sc. Its effect was simulated by reducing the transporters' maximal rate of transport by 90% and the permeability of the basolateral membrane to the Cl^- ion by 85% (DIDS) and 78% (SITS). The variation of the fluxes of the different transport systems after the application of the inhibitor are represented in Table 3, columns 5 and 6.

The effects of DIDS and SITS on *I*sc could only be simulated by increasing the permeability to Na^+ of the apical and basolateral barriers.

The effect of these inhibitors on *I*sc was attributed by Coimbra et al. (1988) to the inhibition of the HCO_3^-/Cl^- exchanger present in the basolateral membrane. Barrias (2003) described the presence of a $Na^+/HCO_3^-/Cl^-$ exchanger also in the basolateral membrane of the cells. As stated, this exchanger is also sensitive to inhibition by SITS and DIDS.

Taking these data into account, we reduced the maximal rate of both these transporters in the simulations and used distinct time constants to achieve more overlapping of the data. It was also necessary to inhibit the Cl^- channels in the basolateral membrane.

Since the alterations induced by the simulation of the effect of both these inhibitors on *I*sc are similar in every aspect, they will be analyzed together. As we can see (Table 3, columns 5 and 6), by reducing the maximal rates of the HCO_3^-/Cl^- ($JCl^-\_HCO_3^-\_Hem$) and $Na^+/HCO_3^-/Cl^-$ ($JNa^+\_HCO_3^-\_Hem$) transporters and the permeability of the specific Cl^- channels on the basolateral barrier (JCl^-_DifHem), there is a direct decrease in the flux of ions via these transport systems. The decrease in the flux of bicarbonate ions from the cell by the HCO_3^-/Cl^- exchanger ($JCl^-\_HCO_3^-\_Hem$) means a rise in the intracellular concentration of bicarbonate and a displacement of the CO_2 hydration reaction to the left (reduction of $JHCO_3^-\_P$) and,

thus, a decrease in the production of H^+ ions. This drop leads to a slight decrease in their exit flux out of the cell because of the lower rate of transport of the Na^+/H^+ exchanger ($JH^+\_Na^+\_Hem$) and of the proton pump (JH^+_P).

Effect of (Dihydronindenyl)oxy Alkanoic Acid on *I*sc

(Dihydronindenyl)oxy alkanoic acid (DIOA) is an inhibitor of the Cl^-/K^+ cotransporter (Linton and O'Donnell 1999; Soler et al. 1993). The effect of this substance on the *I*sc of the OME was described by Rebelo da Costa (1994). Its effect was simulated by reducing the maximal rate of transport of the cotransporter by 95%. The experimental values of *I*sc and those resulting from the simulation are represented in Fig. 3f. Table 3, column 7, presents the variation of the fluxes of the different transport systems after application of the inhibitor.

In order to simulate the effect of DIOA on *I*sc, it was necessary to decrease the permeability to the Cl^- ion of the basolateral membrane and increase the fraction of K^+ ion transported by the K^+/Cl^- cotransporter in the reference condition.

By reducing the maximal rate of transport of the K^+/Cl^- transporter, there is a direct decrease on the efflux of K^+ and Cl^- ions from the cell (Fig. 2f), hence an increase in the diffusional flux of these ions via the specific channels (JCl^-_D and JK^+_D). The increased intracellular concentration of the K^+ ion leads to a slight fall in the rate of transport of the Na^+/K^+ pump and to a depolarization. That implies a slight decrease in the diffusional flux of the bicarbonate ions ($J\ HCO_3^-\_D$), a drop in the intracellular production of the bicarbonate ion ($J\ HCO_3^-\_P$) and a reduction in the rate of transport of the HCO_3^-/Cl^- exchanger ($JCl^-\_HCO_3^-\_Hem$). The decrease in $JHCO_3^-\_P$ also implies a reduced intracellular production of H^+ ions and a reduction in their flux via the proton pump (JH^+_P).

Effect of Ouabain on *I*sc

Ouabain is a specific inhibitor of the Na^+/K^+ pump (Schneider et al. 1998; Shimizu et al. 1983). The effect of this substance on *I*sc when added to the basolateral side of the epithelium was described by Rebelo da Costa et al. (1999a). Its effect was simulated by entering a 95% reduction of the pump's maximal rate of transport. The experimental values and those resulting from the simulation are represented in Fig. 3g. There are no significant discrepancies between the values computed and the experimental values. Table 3, column 8, reports the variation of the fluxes of the different transport systems after application of the inhibitor.

In Table 3, column 8, we can see that by reducing the maximal rate of transport of the Na^+/K^+ pump, there is a direct decrease in the flux of ions via this transport system ($JpNa^+$): the entry of K^+ ions and the exit of Na^+ ions into and from the cell. This decrease entails a reduction in their diffusional fluxes via the specific channels (JNa^+_D e JK^+_D). The sharp increase in the intracellular concentration of the Na^+ ion leads to a decrease in its entry flux by the Na^+/H^+ exchanger ($JH^+\_Na^+\_Hem$) and to the inversion of the fluxes of the $Na^+/HCO_3^-/Cl^-$ transporter ($JNa^+\_HCO_3^-\_Hem$). Since the operation of this pump contributes to the membrane potential, its inhibition leads to a sharp depolarization. This depolarization implies the reduction of the diffusional fluxes of negatively charged ions (JCl^-_D e $JHCO_3^-\_D$) and, hence, an intracellular accumulation of chloride and bicarbonate and a consequent decrease of $J\ HCO_3^-\_P$, an inversion of the fluxes of the $Na^+/HCO_3^-/Cl^-$ transporter and a reduction in the rate of transport of the HCO_3^-/Cl^- exchanger ($JCl^-\_HCO_3^-\_Hem$). The decrease in $JHCO_3^-\_P$ also implies a reduction in the intracellular production of H^+ ions and, thus, a reduction of their flux via the proton pump (JH^+_P).

Effect of Bafilomycin A_1 and Amiloride on pH_i

The strategy used to simulate the effect of bafilomycin and amiloride on pH_i was distinct from that used in the previous simulations. Since the experimental results (Oliveira 2004) were obtained using external solutions without bicarbonate and carbon dioxide ions, we reduced the value of the concentrations of these components in the extracellular solutions prior to doing the simulations so that the model's parameters (permeabilities, affinities, maximum rates, etc.) were always positive.

As well as changing the extracellular concentrations of some components, other modifications had to be introduced in the stationary state in order to render it possible to simulate the effect of both these inhibitors on pH_i. These modifications were introduced to increase the rate of transport of the Na^+/H^+ exchanger and the production of nonvolatile acids. In turn, these changes led to alterations in some of the fluxes in the stationary state of other transport systems (Fig. 3h, i).

The effect of amiloride on pH_i was simulated by reducing the maximal rate of transport of the Na^+/H^+ exchanger and the permeability of the basolateral membrane to the Na^+ ion by 98%. The experimental values and those resulting from the simulation are represented in Fig. 3h. Table 3, column 9, represents the variation of the fluxes of the different transport systems after application of the inhibitor. The effect of bafilomycin A_1 was simulated by reducing the maximal pumping rate of V-ATPase by

99%. The experimental values and those resulting from the simulation are represented in Fig. 3i. Table 3, column 10, represents the variation of the fluxes of the different transport systems after application of the inhibitor.

As we can see in Table 3, columns 9 and 10, the reduction of the maximal rates of transport inhibited in both these simulations, JH^+_PM and $JH^+\_Na^+\_HemM$, produced effects in the final fluxes of the various membrane transporters which were identical to those seen in the simulations of the effect of both compounds on *I*sc.

Discussion

The model presented above is not intended to be a thorough representation of the system it aims to simulate. It deals mainly with the cell mechanisms responsible for the generation of a short circuit current by the OME mounted in vitro under zero voltage-clamp conditions. The model can be modified to compute the behavior under open circuit but in the absence of the corresponding experimental data cannot be evaluated under those conditions. Among these mechanisms there is a very powerful transport of protons toward the extrapaleal compartment, a phenomenon that has been monitored simultaneously and independently (Machado et al. 1990). The model is also an analytical tool that can be used to show the internal coherence of the qualitative model previously proposed (Coimbra et al. 1988).

To build this model it was necessary to introduce some membrane transporters as suggested by the effects of a number of transport inhibitors when applied to the in vitro preparation. In addition, it was necessary to postulate the existence of specific Na^+, K^+, Cl^- and HCO_3^- channels and of a nonvolatile acid/Cl^- exchanger.

The details of the metabolism of these cells are unknown, but Machado et al. (1988) has shown that some of the components of the Krebs cycle activate the *I*sc. The nonvolatile acids were included because their nonexistence was highly unlikely and because their introduction will enable further simulations about their role.

We performed several simulations of protocols verified experimentally. For each case, an analysis was performed not only of the variation in the parameter measured experimentally but also of the variation in the fluxes of the various different transporters.

In all of the simulations performed, it was possible to reproduce the experimental results obtained for the effect of specific inhibitors of transport systems on the *I*sc and on pH_i. In order for this to happen, it was necessary, in some cases, to make alterations to one or more parameters of the reference condition, which may be due to:

- inaccuracy of one or more of the kinetics chosen to stipulate the fluxes of the different transport systems;
- blurring in the model owing to a lack of experimental data which would enable the parameters of the reference condition to be ascertained;
- variations in the preparations used to obtain the different experimental results used in these simulations.

For each simulation carried out, the analysis of the results is consistent. In other words, the results were not ascertained using implausible or impossible values for the different fluxes.

We feel that the estimates which at this time are lacking relate to the time constants of the transients. The model was built in a modular fashion so that it can easily be altered. It therefore enables several distinct experimental situations to be simulated. The model does not include a description of calcium movements. The observations resulting from the work undertaken by Coimbra et al. (1988, 1992) allow us to conclude that calcium ions passively cross the EEM cells. Under short-circuit conditions and in the absence of a transepithelial liquid flux, we are forced to assume that the intracellular calcium is in electrochemical equilibrium with the external calcium. This implies that, for an intracellular potential of around -40 m*V*, the concentration of intracellular calcium is around 20 times higher than the external concentration, which runs counter to the generally accepted concept that intracellular concentrations of calcium are at least three orders of magnitude lower than external ones. Since this is a highly controversial point, it was felt that it would be wise to wait for further observations.

References

Ashe JR Jr, Carter B, Thomas W, Kerr W (1956) Diamox, a carbonic anhydrase inhibitor, as an oral diuretic in pregnancy. Obstet Gynecol 7:242–248

Barrias C (2003) Biomineralização: mecanismos celulares e moleculares de calcificação. Doctoral thesis, ICBAS, Universidade do Porto, Porto

Benos D, Saccomani G, Sariban-Sohraby S (1987) The epithelial sodium channel. Subunit number and location of the amiloride binding site. J Biol Chem 262:10613–10618

Bicho A, Ferreira H, Ferreira K (1999) Chloride channels in the eel intestine. J Exp Biol 202:39–46

Boron W, Boulpaep E (1983) Intracellular pH regulation in the renal proximal tubule of the salamander. Basolateral HCO_3^- transport. J Gen Physiol 81:53–94

Cabantchik ZI, Greger R (1992) Chemical probes for anion transporters of mammalian cell membranes. Am J Physiol 262:C803–C827

Chatterjee D, Chakraborty M, Leit M, Neff L, Jamsa-Kellokumpu S, Fuchs R, Bartkiewicz M, Hernando N, Baron R (1992) The osteoclast proton pump differs in its pharmacology and catalytic subunits from other vacuolar H^+-ATPases. J Exp Biol 172:193

Coimbra J, Machado J, Fernandes P, Ferreira H, Ferreira K (1988) Electrophysiology of the mantle of *Anodonta cygnea*. J Exp Biol 140:65–88

Coimbra A, Fernandes P, Ferreira K, Ferreira H (1992) Intracellular calcium in the cells of the outer mantle epithelium of *Anodonta cygnea*. Comp Biochem Physiol A 103:497–500

Coimbra A, Ferreira K, Fernandes P, Ferreira H (1993) Calcium exchanges in *Anodonta cygnea*: barriers and driving gradients. J Comp Physiol [B] 163:196–202

Drose S, Altendorf K (1997) Bafilomycins and concanamycins as inhibitors of V-ATPases and P-ATPases. J Exp Biol 200:1–8

Ehrenfeld J, Garcia-Romeu F, Harvey B (1985) Electrogenic active proton pump in *Rana esculenta* skin and its role in sodium ion transport. J Physiol 359:331–355

Enns T, Hill EP (1983) CO_2 diffusing capacity in isolated dog lung lobes and the role of carbonic anhydrase. J Appl Physiol 54:483–490

Gluck S (1992) V-ATPases of the plasma membrane. J Exp Biol 172:29–37

Grinstein S, Smith J (1987) Asymmetry of the Na^+/H^+ antiport of dog red cell ghosts. Sidedness of inhibition by amiloride. J Biol Chem 262:9088–9092

Hoffman PG, Tosteson DC (1971) Active sodium and potassium transport in high potassium and low potassium sheep red cells. J Gen Physiol 58:438–466

Hudson R (1992) Ion transport by the isolated mantle epithelium of the freshwater clam, *Unio complanatus*. Am J Physiol 263: R76–R83

Hudson R (1993) Bafilomycin-sensitive acid secretion by mantle epithelium of the freshwater clam, *Unio complanatus*. Am J Physiol 264:R946–R951

Jensen BL, Skott O (1996) Blockade of chloride channels by DIDS stimulates renin release and inhibits contraction of afferent arterioles. Am J Physiol 270:F718–F727

Linton S, O'Donnell M (1999) Contributions of K^+:Cl^- cotransport and Na^+/K^+-ATPase to basolateral ion transport in malpighian tubules of *Drosophila melanogaster*. J Exp Biol 202:1561–1570

Ludens J, Fanestil D (1972) Acidification of urine by the isolated urinary bladder of the toad. Am J Physiol 223:1338–1344

Machado J, Ferreira KG, Ferreira HG, Coimbra J (1988) Substracte activation of the short-circuit current of outer mantle epithelium of *Anodonta cygnea*. Comp Biochem Physiol A Physiol 91: 487–492

Machado J, Ferreira K, Ferreira H, Fernandes P (1990) The acid-base balance of the outer mantle epithelium of *Anodonta cygnea*. J Exp Biol 150:159–169

Mahnensmith R, Aronson P (1985) Interrelationships among quinidine, amiloride, and lithium as inhibitors of the renal Na^+–H^+ exchanger. J Biol Chem 260:12586–12592

Maren TH (1967) Carbonic anhydrase: chemistry, physiology, and inhibition. Physiol Rev 47:595–781

Markovich D (2001) Physiological roles and regulation of mammalian sulphate transporter. Physiol Rev 81:1499–1533

Mason NP, Petersen M, Melot C, Imanow B, Matveykine O, Gautier M-T, Sarybaev A, Aldashev A, Mirrakhimov MM, Brown BH, Leathard AD, Naeije R (2003) Serial changes in nasal potential difference and lung electrical impedance tomography at high altitude. J Appl Physiol 94:2043–2050

Murer H, Hernando N, Forster I, Biber J (2000) Proximal tubular phosphate reabsorption: molecular mechanisms. Physiol Rev 80:1373–1409

Oliveira CPF (2004) Transporte iónico em *Anodonta cygnea*. Doctoral thesis, ICBAS, Universidade do Porto, Porto

Oliveira PF, Lopes IA, Barrias C, Rebelo da Costa AM (2004) H^+-ATPase of crude homogenate of the outer mantle epithelium of *Anodonta cygnea*. Comp Biochem Physiol A Mol Integr Physiol 139:425–432

Pace CS, Tarvin JT, Smith JS (1983) Stimulus–secretion coupling in beta-cells: modulation by pH. Am J Physiol 244:E3–E18

Rebelo da Costa A (1994) Movimentos de Cálcio em *Anodonta cygnea*. Doctoral thesis, ICBAS, Universidade do Porto, Porto

Rebelo da Costa A, Barrias C, Oliveira P, Ferreira H (1999a) The Na^+-K^+ ATPase in the outer mantle epithelium of *Anodonta cygnea*. Comp Biochem Physiol A Mol Integr Physiol 122:337–340

Rebelo da Costa A, Oliveira P, Barrias C, Ferreira H (1999b) Identification of a V-type ATPase in the outer mantle epithelium of *Anodonta cygnea*. Comp Biochem Physiol A Mol Integr Physiol 123:337–342

Schneider R, Wray V, Nimtz M, Lehmann WD, Kirch U, Antolovic R, Schoner W (1998) Bovine adrenals contain, in addition to ouabain, a second inhibitor of the sodium pump. J Biol Chem 273:784–792

Shimizu T, Nakanishi T, Uemura S, Jarmakani JM (1983) Effect of hypoxia on ouabain inhibition of sodium pump in newborn rabbit myocardium. Am J Physiol 244:H756–H762

Soler A, Rota R, Hannaert P, Cragoe E Jr, Garay R (1993) Volume-dependent K^+ and Cl^- fluxes in rat thymocytes. J Physiol 465:387–401

Steinmetz P, Andersen O (1982) Electrogenic proton transport in epithelial membranes. J Membr Biol 65:155–174

Stephen HW, Dantzler WH (2003) Molecular and cellular physiology of renal organic cation and anion transport. Physiol Rev 84:987–1049

Van Slyke D, Sendroy J (1928) Studies of gas and electrolyte equilibria in blood. J Biol Chem 79:739–819